Beijing Tau-Charm Factory Workshop'96, Beijing, China, Feb. 5-9, 1996

DAΦNE Impedance Study

M. Zobov, R. Boni, A. Gallo, A. Ghigo, F. Marcellini,
M. Migliorati, L. Palumbo, M. Serio, B. Spataro

INFN-LNF, C.P. 13, 00044 Frascati (Roma), Italy

ABSTRACT

We discuss contributions of various DAΦNE vacuum chamber elements to the beam coupling impedance and describe some novel design solutions allowing to reduce both the broad-band impedance and the high order mode (HOM) content.

INTRODUCTION

The double ring electron-positron collider DAΦNE [1] is presently under construction at LNF in Frascati (Italy). It is designed to reach a maximum luminosity of $5.3 \cdot 10^{32}$ $cm^{-2}s^{-1}$ at the energy of Φ resonance (1020 Mev in the center of mass). Table 1 shows relevant parameters of the DAΦNE main rings.

In order to achieve the required luminosity a large total current, up to 5.2 A, distributed over 120 bunches (maximum) has to be stored in each ring. This gives rise to the problem of the parasitic electromagnetic interaction of the beam with the surrounding vacuum chamber. Much care has been taken in the designing of the DAΦNE vacuum chamber elements to reduce the machine coupling impedance, i. e. to avoid excessive beam power loss and minimize instability phenomena due to the interaction.

In this paper we briefly discuss the design of the main DAΦNE vacuum chamber components with analysis of their coupling impedance and measures undertaken to reduce it.

DAΦNE RF CAVITY

Cavity Shape

The power requirement is quite moderate for the RF cavity. The necessary RF power per ring, given by the sum of the power delivered to the beam and that dissipated on the cavity walls, is about 100 kW for 120 bunches at 250 kV gap voltage. One 150 kW klystron amplifier per ring will be installed to feed the 368 MHz RF cavity.

In the cavity shape choice the goal was to reduce both the shunt impedance R and the (R/Q) of the cavity HOMs in order to increase the multibunch instability thresholds. The main cavity body has been choosen to have "rounded" profile mainly due to a simpler mechanical realization. The basic ideas to reduce the HOM impedances were to provide large and long cavity tubes to let the parasitic modes propagate along them and to couple out the HOM energy by means of waveguides (WG) [2]. Fig.1 shows a sketch of the DAΦNE RF cavity.

The cavity shape was then optimized in order to keep the fundamental mode (FM) impedance above 3 MΩ to reduce the dissipated power and make the cooling design easier. Much care was also taken to keep the higher impedance HOM frequencies far away from harmonics of the beam in order to avoid resonant enhancement of the parasitic power loss.

Table 1. Main DAΦNE parameters

Energy	E	510.0	Mev
Average radius	R	15.548	m
Emittance	ε_x / ε_y	1/0.01	mm·mrad
Beam-beam tune shift	ξ_x / ξ_y	0.04/0.04	
Betatron tune	ν_x / ν_y	5.09/6.07	
RF frequency	f_{rf}	368.32	MHz
Harmonic number	h	120	
Revolution frequency	f_0	3.0688	MHz
Max. number of bunches	n_b	120	
Minimum bunch separation	s_b	81.4	cm
Bunch average current	I_0	43.7	mA
Particles per bunch	N	$9.0 \cdot 10^{10}$	
Momentum compaction	α	0.02	
Natural energy spread	$\sigma_{\varepsilon 0} / E$	0.000396	
Bunch length	σ_z	3.0	cm
Synchrotron radiation loss	U_0	9.3	keV/turn
Damping time	τ_ε / τ_x	17.8/36.0	ms
RF voltage	V_{rf}	250	kV
Synchrotron tune	ν_s	0.0078	
Beta functions at IP	β_x^* / β_y^*	450/4.5	cm
Maximum luminosity	L	$5.3 \cdot 10^{32}$	$cm^{-2}s^{-1}$

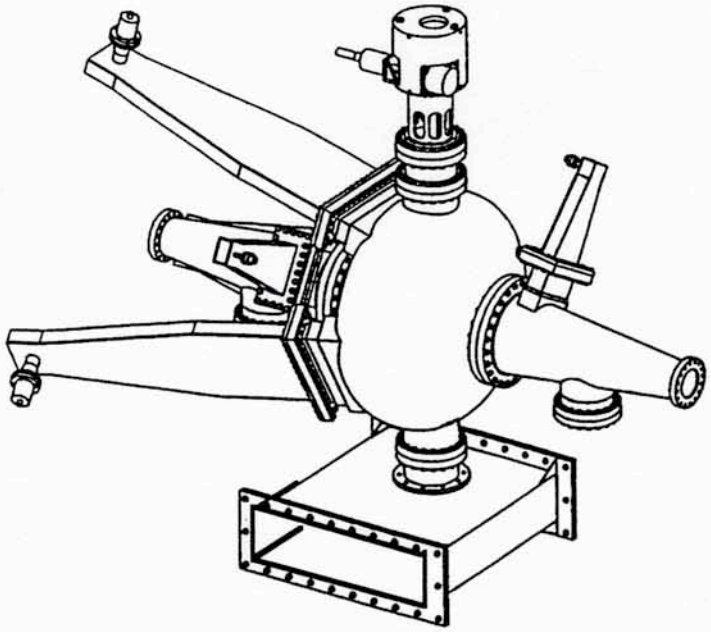

Figure 1. DAΦNE RF cavity sketch.

HOM Damping and Measurements

HOM damping is obtained by opening rectangular slots onto the cavity surface and applying at those positions rectangular WGs which can convey out of the cavity the fields of the parasitic modes in the TE10 WG dominant mode.

The DAΦNE cavity is equipped with five WGs. Three WGs are applied, 120° apart for symmetry considerations, onto the central body. They are 305x40 mm^2 rectangular WGs with TE10 cut-off at 495 MHz. Their position allows, on the average, the best coupling with the magnetic field H_Φ of the HOMs. One additional 140x40 mm^2 WG, with cut-off at 1070 MHz, is placed on each tapered tube to couple some high frequency HOMs which penetrate along the pipes and have intense H_Φ at that position.

A comprehensive analytical and numerical study has been performed [3] showing considerable reduction of the parasitic mode quality factors Q due to the WGs.

In order to dissipate the HOM power extracted from the cavity, the rectangular WGs are converted in double ridge WGs with a smooth and wideband tapered section which is finally adapted to 50 Ω by a transition to coaxial. The obtained bandwidth is 0.5-3 GHz and 1.2-3 GHz respectively with standing wave ratio (VSWR) < 2 in the full band. Then, by means of coaxial vacuum feedthroughs, the HOM power can be dissipated onto external 50 Ω loads in air [4]. In this way, the application of dissipating materials in ultra high vacuum (UHV) is avoided. Moreover the HOM power can be monitored.

Table 2 shows the results of FM and HOM parameter measurements on a copper cavity prototype equipped with the WGs. The last column in Table 2 gives the coupled bunch instability rise time in case of full coupling with the damped HOMs.

As it can be seen, with the use of the described damping system, the parasitic mode quality factors Qs of the most dangerous HOMs are reduced, on the average, by two orders of magnitude. In some cases, like for the TM011, the Q damping is even stronger. The FM quality factor decreases by 12 % due to the application of WGs.

The beam power delivered to the cavity HOMs estimated for the 30 bunches initial operation of DAΦNE is about 200 W. In the case of full current operation, the HOM losses are below 1 kW per WG.

Table 2. Cavity Prototype Modes

Mode	Freq. (MHz)	R/Q (Ω)	Undamped Q	WG damped Q	τ (ms)
0-EM-1	357.2	61	25000	22000	
0-MM-1	745.7	16	24000	70	1.4
0-EM-2	796.8	0.5	40000	210	14.9
0-MM-2	1023.6	0.9	28000	90	17.5
0-EM-3	1121.1	0.3	12000	300	15.4
0-MM-3	1175.9	0.6	5000	90	25.6
0-EM-4	1201.5	0.2	9000	180	38.4
0-EM-5	1369.0	2.0	5000	170	4.1
0-MM-4	1431.7	1.0	4000	550	2.6
1-MM-1 a	490.0	5.1*	30500	650	3.0
1-MM-1 b	491.3	5.1*	28500	830	2.4
1-EM-1 a	523.5	14.0*	31500	150	4.5
1-EM-1 b	549.7	14.0*	32000	50	13.1

(*) Normalized impedance, URMEL definition.

Present Status

The first RF cavity, equipped with 3 HOM waveguide absorbers (See Fig. 2) has been successfully tested in the beginning of April 1996. During one day of RF conditioning the input power was rised up to 22 kW/cw for a gap voltage of 300 kV-peak, which is more than required for the DAΦNE operation. The measured quality factor of the cavity is 33000. No multipactoring or discharges occurred during the tests. The second cavity will be delivered in fall 1996.

LONGITUDINAL FEEDBACK KICKER

Despite the HOMs are heavily damped in the RF cavity, the probability of coupling of a coupled bunch mode spectrum line to a damped HOM is high and, due to the high beam current, the growth time of unstable modes can be substantially shorter than the radiation damping time.

The required additional damping is provided via a time domain bunch by bunch feedback system based on digital signal processors [5]. The feedback chain ends with the longitudinal kicker, an electromagnetic structure capable to transfer the proper longitudinal momentum correction to each bunch.

The following main requirements were taken into account while designing the DAΦNE longitudinal feedback kicker: high shunt impedance, i. e. kicker efficiency; large bandwidth necessary to cover all possible coupled bunch modes; absence of parasitic HOMs which can further excite multibunch instabilities.

Design of Overdamped Cavity

The longitudinal kicker design is based on a waveguide overloaded cavity [6]. Fig.3 shows an exploded view of the cavity.

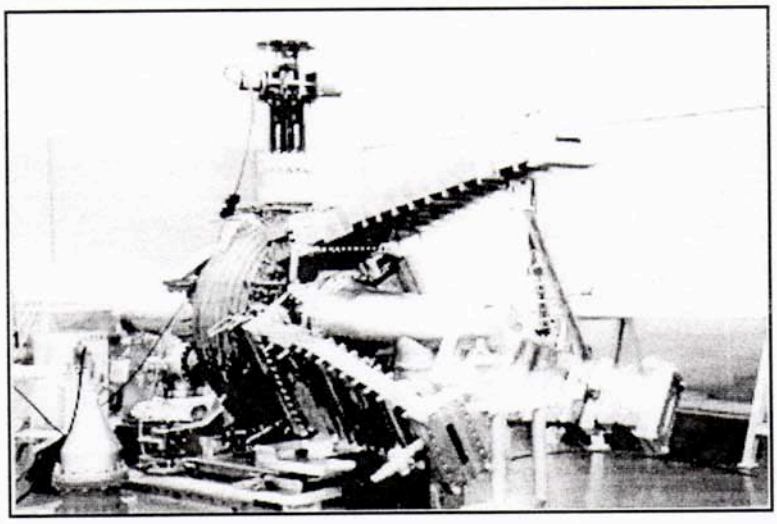

Figure 2. DAΦNE RFcavity under test.

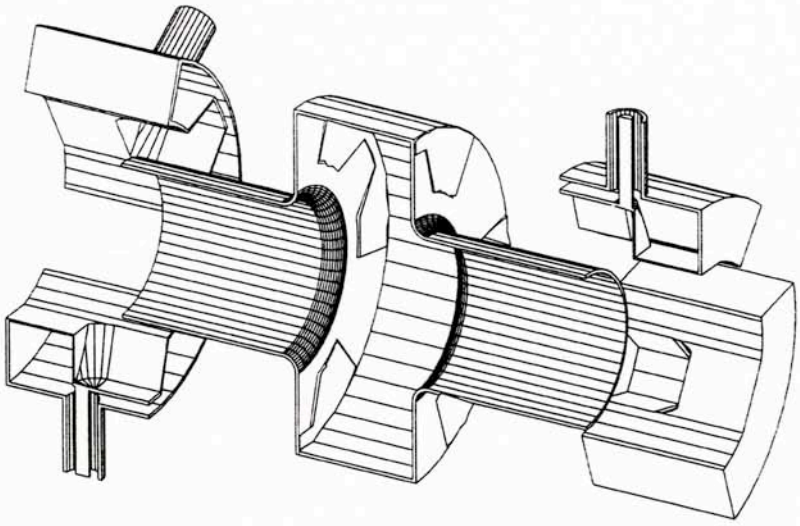

Figure 3. Exploded cut view of the kicker cavity

The idea of using an RF cavity as a longitudinal kicker is based on some simple considerations. When all the RF buckets are filled, all possible coupled bunch modes are present in a frequency span between nf_{RF} and $(n\pm1/2)f_{RF}$, with n any integer and f_{RF} the bunch frequency. Therefore, the minimum bandwidth requirement for the longitudinal kicker is $f_{BW}=f_{RF}/2$, as long as the response is centered onto $f_c=(n\pm1/4)f_{RF}$ [7]. A center frequency $f_c = 3.25\ f_{RF} \approx 1197$ MHz has been chosen, so that the resulting loaded quality factor of the cavity has to be set to about $Q_L = f_c / f_{BW} \approx 6.5$. Therefore, if the damping waveguides are symmetrically placed with respect to the fundamental mode field distribution and half of them are used as input ports while the remaining as matched terminations, the external Q values are given by:

$$Q_{ext_{inp}} = Q_{ext_{out}} = Q_L = 13 \tag{1}$$

The R/Q factor of a pill-box cavity resonating around 1.2 GHz with stay-clear apertures of 88 mm is limited to about 60 Ω. The kicker shunt impedance R_s has a peak value given by:

$$R_s = V_g^2 \,/\, 2P_{in} = (R/Q)Q_{ext_{out}} \approx 780\Omega \tag{2}$$

This means that the attainable shunt impedance is about twice the value of a two-electrodes stripline module [8], while no HOMs are likely to remain undamped in this structure.

The coupling waveguide is a single ridged like waveguide with 6 mm gap to lower the TE10 cutoff frequency down to 690 MHz. The waveguide-to-coaxial transition is designed with the same criteria adopted for the main ring accelerating cavity [4]. The coaxial size is the standard 50 Ω 7/8" which can withstand more than 1 kW power flow. Moreover, we can use for this coaxial standard the broadband ceramic feedthrough already developed for the transitions of the main ring cavity [9].

Simulation and Experimental Results

Numerical simulations for the structure shown in Fig. 3 have been performed with the 3D code HFSS [10]. From the computed transmission coefficient S21 between the three input and the three output ports we observe that the central frequency of the kicker cavity fundamental mode is about 1215 MHz with a 3 dB bandwidth of 220 MHz. This agrees well with the results of measurements on the kicker prototype (see Fig.4).

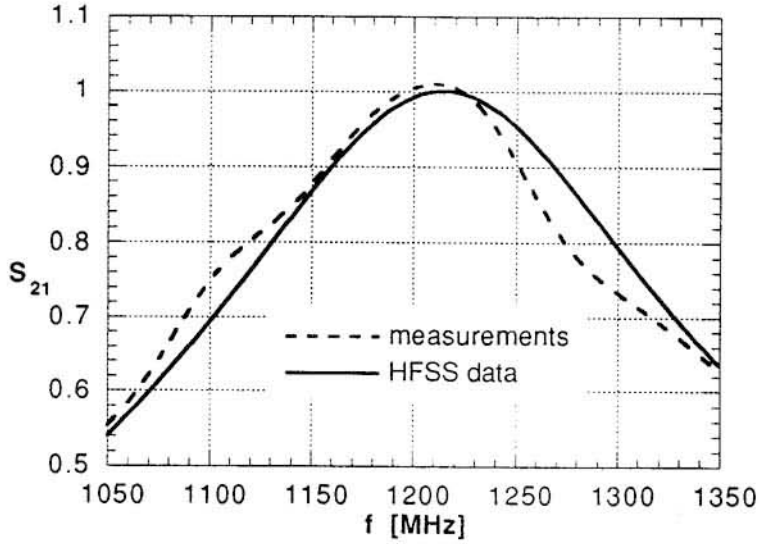

Figure 4. Theoretical and experimental kicker frequency response.

All the HOMs below the beam pipe cut-off frequency appear extremely damped so that they are not considered dangerous for the longitudinal and transverse beam dynamics.

In order to calculate the kicker shunt impedance, the gap voltage has been obtained by post-processing the field solution given by the 3D simulator. This yielded the impedance peak value of about 750 Ω, which is in a good agreement with the rough estimate of eq. 2.

The longitudinal beam coupling impedance $Z_l(\omega)$ has been measured with the wire method. A 3 mm diameter copper wire has been inserted in the cavity along the beam axis and connected to a 50 Ω line through a resistive matching network. The coaxial wire-beam tube system is a Z_0'=203 Ω transmission line. Then, according to [11] the coupling impedance can be estimated as:

$$Z_l(\omega) = 2Z_0'\left(\frac{1}{S_{21}} - 1\right) \tag{3}$$

where S21 is the complex transmission coefficient between the two wire ports measured by a Network Analyzer calibrated to take into account the cable and matching network attenuations, as well as the linear phase advance due to the electrical length of the device. The coupling impedance turns out to be approximately by a factor of 2 smaller of the kicker shunt impedance.

At present we have two kickers ready to be installed in the main rings. The measured shunt impedance of the real kickers (620 Ω) is somewhat lower than the value we have got in the simulations and measurements on the prototype, but the bandwidth is proportionally larger, i. e. R/Q = 57 Ω is the same value as obtained in the simulations. Preliminary experiments have shown that by introducing some small mismatches into each coaxial line we have a possibility to increase the shunt impedance at the expense of bandwidth reduction, if necessary.

TRANSVERSE FEEDBACK KICKER

The DAΦNE transverse feedback system must provide damping of the resistive wall instability and the control of a large number of transverse coupled bunch modes.

Two transverse kickers, one for the horizontal and another one for the vertical plane, will be installed in each ring. The transverse kicker is a conventional stripline pair (see Fig.5).

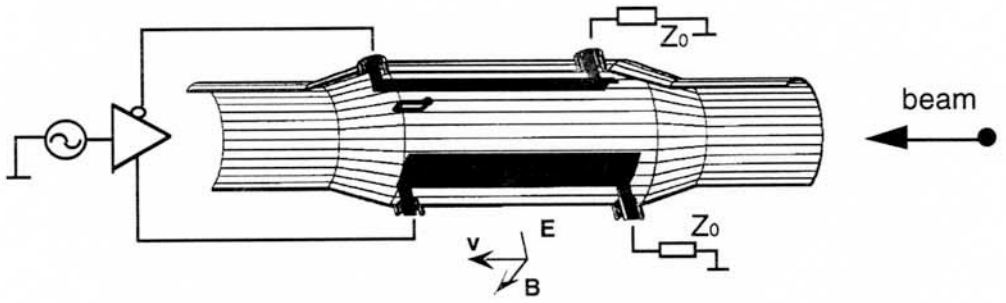

Figure 5. Transverse kicker: cut view and working scheme.

Design and Efficiency

The electromagnetic design has been carried out mainly by means of the HFSS code using a "cut and try" procedure to achieve good performances of the kicker within the machine constraints.

The kickers are based on a pair of striplines (20 cm length, 1 mm thickness). The stay clear aperture of the device is that of the rest of the straight section beam pipe (88 mm), and the vacuum chamber diameter in the kicker section is 120 mm. Two tapers, 50 mm long, joining the kicker vacuum chamber to the rest of the beam pipe, are also needed in order to minimize the losses. We found that if 80° is the stripline coverage angle, each electrode forms with the vacuum pipe a transmission line of Z_0=50 Ω characteristic impedance. Two standard 7/8" coaxial feedthroughs connect the electrode ends with the amplifier and the external load. The final geometry of the coax line-stripline transition minimizes the reflected power (less than 6% of the forward one in the operating bandwidth) to the amplifier.

The kicker efficiency is described by the transverse shunt impedance parameter $R_\perp$ which can be calculated accordingly to the following formula [8]:

$$R_\perp = 2Z_0\left(\frac{g_{trans}}{kh}\right)^2 \sin^2(kl) \qquad (4)$$

where g_{trans} is the coverage factor ($g_{trans} \approx 1$), k=ω/c, h is the stay clear radius and l the electrode length.

The results given by the previous formula can be compared to those obtained from the integration of the electric and magnetic fields on the kicker axis as computed by the simulation code. Fig. 6 shows this comparison.

A peak value larger than 2 KΩ together with a bandwidth wider than 300 MHz has been obtained. As a first estimate, a kicker driving power of ≈200 W seems enough to keep the machine transverse instabilities under control [12].

Coupling Impedance and Power Losses

A simulation of the measurement with a metallic wire placed along the kicker axis, simulating the beam, has been performed. The longitudinal coupling impedance and the transfer impedances of the kicker, defined as the ratio of the voltages at the output ports to the beam current [13], were calculated.

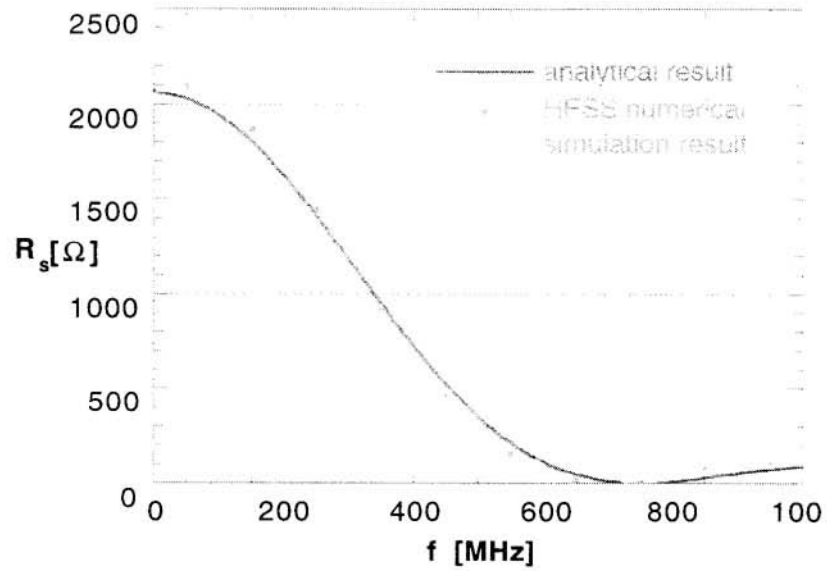

Figure 6. Transverse shunt impedance.

Coupling and transfer impedances can be easily obtained from the scattering matrix yielded by HFSS simulations according to eq.3 and the following formula:

$$Z_{tr,i} = \frac{S_{2i}}{S_{21}} 2\sqrt{Z_0 Z_0'} \tag{5}$$

where the subscript i refers to one of output ports (loop, downstream or upstream ports), the input port for the beam is port 2, Z_0 and Z_0' are respectively the characteristic impedance of the output ports (≈50 Ω) and that of the wire beam tube coaxial line (≈130 Ω). The real part of these functions vs. frequency is shown in Fig. 7.

As it can be checked, the coupling impedance at low frequencies in Fig.7 can be reasonably well fitted by the corresponding analytical formula given in Ref. [14].

The beam passage through the kicker structure can excite HOMs that are potentially sources of coupled bunch instability. Using MAFIA [15] and HFSS codes we have found only two trapped modes resonating at 2275 MHz and 2530 MHz.

In order to damp them, two identical rectangular loops have been introduced in the vacuum chamber near the tapers, rotated by 90 degrees with respect to the input ports. The choice of the loop shape and position have been optimized after several HFSS runs.

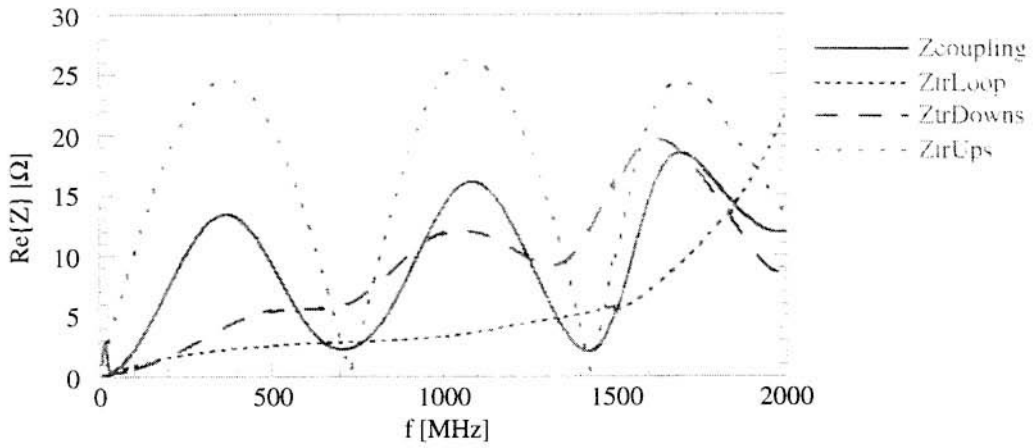

Figure 7. Transverse kicker coupling and transfer impedances (real part).

The values of the loaded Q and R/Q factors for the two mentioned modes are not considered dangerous anymore for the longitudinal beam dynamics.

Knowledge of the coupling and transfer impedances helps to estimate the total power released by the beam to the structure as well as the power flowing in the coaxial lines connected with loops and striplines. The result of the estimates are summarized in Table 3.

The chosen sizes of the striplines and feedthroughs are completely sufficient to manage the power released by the beam together with the incoming power from the endstage amplifier of the transverse feedback system.

BROAD-BAND BUTTON ELECTRODES

Requirements and Design

The beam position monitor (BPM) system is the primary diagnostic system in the DAΦNE main rings. We have 38 BPMs in each ring and 12 in the common part of the interaction regions. They consist of four "button" electrodes mounted flush with the vacuum pipe. In all of them the same type of electrode (SMA 50-MB from Ceramex, France) is used, but, since the vacuum chamber cross-section is largely variable along the ring circumference, we have developed several different designs with different values of the transfer impedance according to the vacuum chamber geometry.

In addition to the measurement of the stationary closed orbit, done with narrow-band detectors, we need other special button monitors to measure the individual time and x/y position offset, on a bunch by bunch basis, i. e. without "memory" of the preceding bunch, in the front-end section of the longitudinal and transverse feedback systems. These monitors are to be placed in the non-intersecting straight sections.

The total number of such special button electrodes is 12 per ring. They must satisfy the following compromising requirements:

- to have a reasonably high transfer impedance Z_{tr}, free from narrow-band resonances in the frequency range of utilization: the necessary design value for DAΦNE is 0.3-0.4 Ω in the region 1300-2000 MHz, to be compared to ~ 0.2 Ω of the ordinary BPM electrodes in the same section;
- to keep the beam coupling impedance within acceptably low values.

The proposed design [16], shown in Fig.8, meets both the requirements. The button itself has a radius r of 7.5 mm and a thickness t of 3 mm, the annular gap w is of 1 mm wide. The dielectric material with relative dielectric constant $\varepsilon \sim 5.2$ is mainly used to fix the button and creates a short piece of the transmission line with $R_0 = 50\ \Omega$. A tapered transition has also the characteristic impedance of 50 Ω and provides matching between the button and the external coaxial connector.

Table 3. Estimated Beam Power Distribution on Transverse Kicker Parts

Number of regularly spaced bunches	**30**	**120**
Total beam released power [W]	372+60*	1483+436*
Power flowing through each loop port [W]	9+30*	40+218*
Power flowing through each downstream port [W]	34	135
Power flowing through each upstream port [W]	143	555
Dissipated power on aluminum walls [W]	≈ 0	23
Power flowing from each downstream port to each upstream port due to amplifier [W]	100	100

*power due to HOMs impedance.

Transfer and Coupling Impedances

The button electrode is mainly sensitive to the beam electric field. The usual equivalent circuit representation of an electrostatic monitor is a generator of the same value of the image current intercepted fraction, shunted by the electrode capacitance to ground. If the button is connected to the detector circuit by means of a short run of coaxial cable having characteristic impedance R_0 and terminated into an R_0 resistor, the transfer (signal) impedance for a centered beam can be written as [16]:

$$Z_{tr}(\omega) = \phi R_0 \frac{j\omega / \omega_2}{1 + j\omega / \omega_1} \tag{6}$$

where $\omega_1 = 1/R_0C_b$ and $\omega_2 = c/2r$, with C_b the button capacitance to ground, r the button radius, c speed of light, ϕ the coverage factor = r/4b and b the beam pipe radius.

Following the arguments of [17], the low frequency component of the longitudinal coupling impedance (per button) can be written as:

$$Z_l(\omega) = \phi\left(\frac{\omega_1}{\omega_2}\right) Z_{tr} \tag{7}$$

In order to estimate the transfer and coupling impedance of the button and compare to the above expressions we have simulated with HFSS the measurement method based on a coaxial wire put along with the beam tube. Eq. (3) and eq. (5) have been used to calculate the coupling (Fig.9) and transfer impedance (Fig.10), respectively.

As it can be seen, the transfer impedance of ~ 0.43 at the working frequency is higher than the necessary value of 0.3-0.4 Ω. It turns out that at low frequencies the numerical curves can be well approximated by the analytical formulae (6) and (7) with $C_b = 3.6$ pF.

It has been found that the first resonant peak observed at 5.2 GHz corresponds to the parasitic HOM trapped around the button. This mode appears to be of TE110 type. All the HOMs are situated beyond the 3 cm bunch spectrum, therefore do not contribute to the beam power losses. Having rather small values of the shunt impedance neither they are dangerous to the multibunch instabilities.

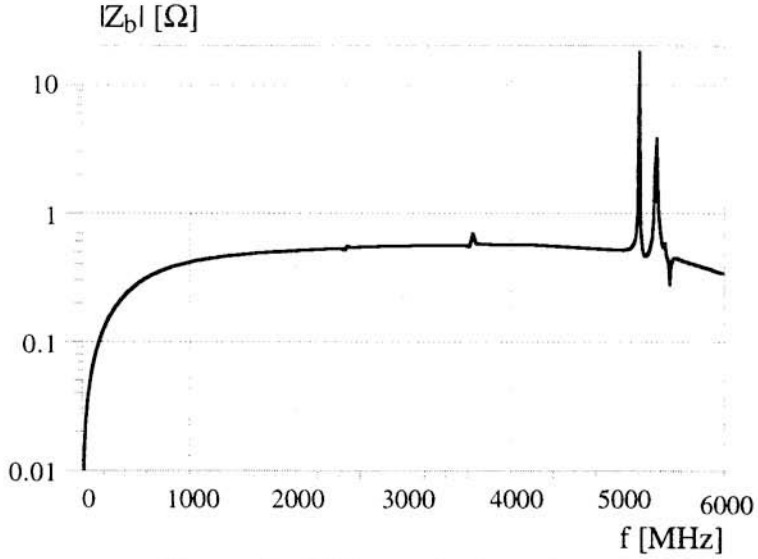

Figure 10. BPM transfer impedance

SHIELDED BELLOWS

The bellows placed between the DAΦNE arcs and straight sections must allow 35 mm longitudinal expansion and 10 mm horizontal offset during the vacuum chamber bake-out. It was decided to avoid any sliding contacts in the bellows screen which could be burned out due to the high image current. Moreover, if, for any reason, there is no contact between the sliding surfaces the capacitance between the sliding contacts can create a resonant cavity with the rest of the bellows. This can affect the multibunch beam stability and is a source of possible high power loss. Another potential danger is creation of dust particles between the sliding surfaces.

Design of Bellows Screen

The bellows screen is made of thin (0.2 mm) strips oriented in the vertical plane and separated by 4 mm gaps (see Fig.11, a). The width of a strip is 5 mm, i. e. wider than the gap between the strips in order to attenuate radiation outside the screen.

The strips are produced by a hot forming method and have a waved shape. This allows the longitudinal expansion. In the working regime the strips are almost straight.

In order to push the HOMs frequencies beyond the bunch spectrum, i. e. to avoid dangerous power losses, it was proposed to put transverse connections between nodes of the waved strips as shown in Fig. 11, b. In this way we reduce the length of the slots created between each neighboring strips. It means that TM waveguide modes with wavelength $\lambda > 2l$, where l is the reduced slot length, can not penetrate outside the screen and excite resonant HOMs. As far as the connections are placed between the nodes the flexibility of the screen does not change much. However, due to the fact that the bellows are placed between the arc and straight section, there are two lateral slots along the screen which are foreseen for the synchrotron radiation exit. It is clear *a priori* that some modes are left in the structure.

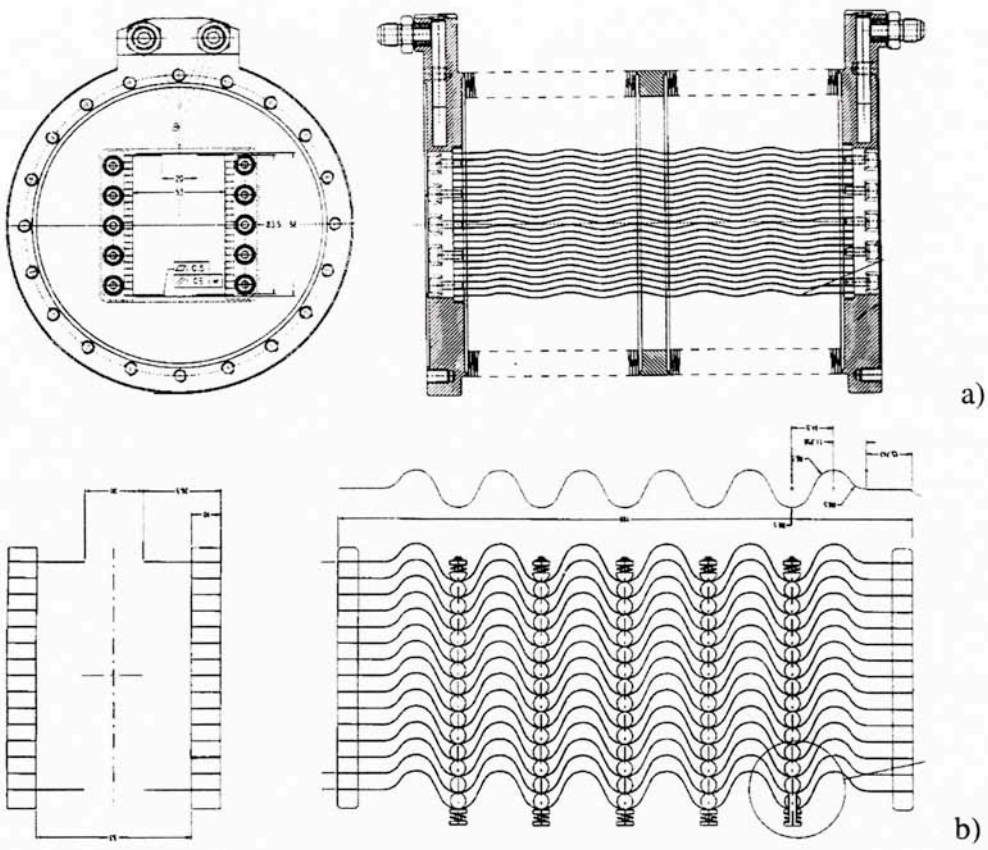

Figure 11. Shielded bellows design: a) bellows and screen without transverse connections; b) screen with transverse connections

In order to damp the remaining modes we propose in addition to the transverse connections to use transverse plates as shown in Fig.12. In order to fit the bellows shape the plates have been chosen to have the "half of the moon" shape. In our understanding these plates push the electric fields of the coaxial type modes further from the beam axis thus reducing the coupling of these modes to the beam. The second advantage is that the plates prevent penetration of the TE modes into the outer volume. Third, the plates can be considered as radiators which help to dissipate the lost power.

Bellows Coupling Impedance

In order to check the effectiveness of the screen, impedance measurements and numerical simulations with MAFIA and HFSS have been carried out [19].

The first impedance measurements have been performed on a prototype with the screen which had neither the transverse connections nor the transverse plates. Figure 13 shows the results of the impedance measurements. Dotted lines correspond to HOMs trapped in the bellows volume without the screen, while solid ones show the shunt impedance of the HOMs remaining in the structure with the inserted screen.

Some observations can be done by analyzing the results presented in Fig.13. First, the HOMs of the cavity itself having shunt impedances up to $10^5\ \Omega$ are successfully eliminated by the screen. On the other hand, the screen introduces new HOMs. Some of them are at very low frequencies.

The frequencies of the new modes appear to cluster around frequencies f = nc/2l, where n = 1,2,3,.. and l is the strip length. Even though the shunt impedances are very low the rise time of the multibunch instabilities due to the modes is at a manageable limit of the DAΦNE longitudinal feedback system. Moreover, the number of the modes is high and the frequency distribution is rather dense. This means that probability of the coupling of the power spectrum lines to the HOMs is not negligible. The power loss in case of the full coupling can be of the order of some thousand watts.

After insertion of the transverse connections and transverse plates the number of remaining modes has been drastically reduced and their impedance has substantially decreased. Table 4 summarizes the measured HOM parameters and the estimated longitudinal multibunch instability rise times for 217 mm bellows length (maximum expansion is 230 mm).

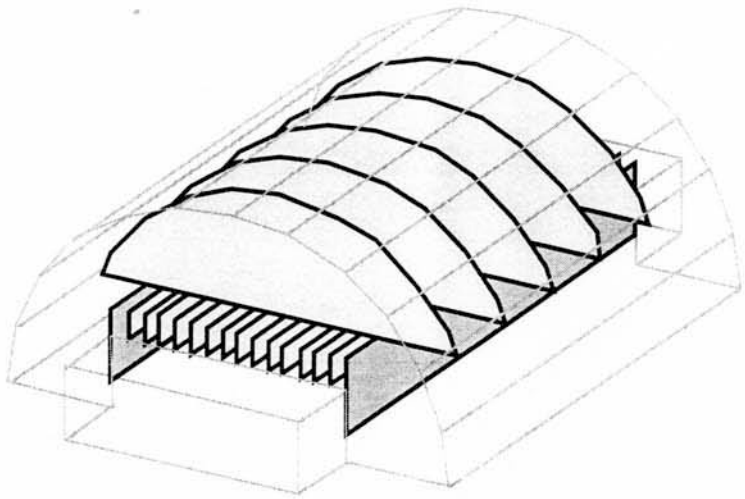

Figure 12. Sketch of the bellows shield with transverse plates (half of the structure)

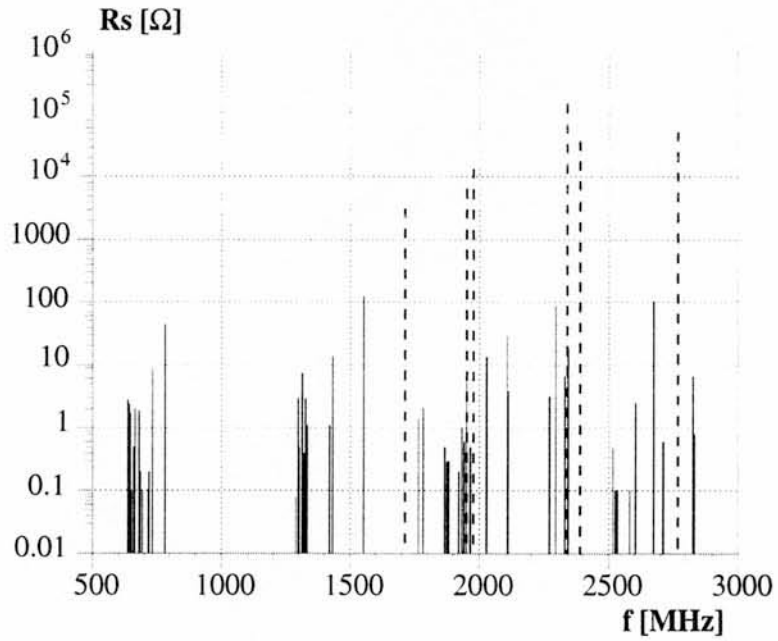

Figure 13. Shunt impedance of measured bellows prototype HOMs.

As it can be seen, the rise time is higher than the radiation damping time which is equal to 17.8 ms for DAΦNE. Remembering that there are 8 bellows in each ring one could expect a proportional reduction of the rise time. However, we believe that all the bellows will be differently expanded, i.e. it is hardly possible that all the frequencies of the HOMs having similar field configuration in different bellows coincide exactly. Nevertheless, if this happens the multibunch instability rise time will be still longer than the damping time provided by the feedback system.

In order to estimate the losses in the worst case let us consider the full coupling (hardly possible) of the mode at 974.8 MHz with a bunch power spectrum line for 120 equally spaced bunches. It gives 85 W. This is a quite acceptable value. We should also stress here that not all the power is dissipated under vacuum. Due to the coaxial nature of the remaining modes a part of the power is dissipated on the bellows surface on air.

Table 4. Measured HOMs in structure containing transverse connections and transverse plates

mode	f [MHz]	Rs [Ω]	τ [ms]
1	667.0	0.8	258.9
2	954.1	1.3	132.5
3	974.8	2.2	77.8
4	1511.8	0.9	191.2
5	1528.5	----	
6	1750.2	0.8	233.5
7	2415.9	6.5	40.7
8	2482.4	----	
9	2645.8	1.9	159.0
10	2681.2	5.8	53.2
11	2906.8	0.6	585.3

CONCLUSIONS

In this paper we describe the design and present status of the DAΦNE vacuum chamber components which were of our main concern from the beam coupling impedance point of view. Here we pay main attention to the novel design features of the components which allow to avoid excessive power loss, substantially reduce the number of trapped HOMs and, consequently, to damp them.

The impedance study of other, more conventional vacuum chamber discontinuities, like tapers, pumping slots etc. can be found, for example, in [20].

REFERENCES

[1] "DAΦNE Machine Project", Contributions to EPAC 94, London, 1994, LNF-94/055(P)

[2] S. Bartalucci et al., "Analysis of Methods for Controlling Multibunch Instabilities in DAΦNE", Particle accelerators, Vol. 48, 4 (1995), pp. 213-237.

[3] S. De Santis et al., "Evaluation of the beam-coupling impedances of the DAΦNE cavity: numerical and analytical results", Nuclear Instruments and Methods in Physics Research, A 366, (1995), pp. 53-59.

[4] R. Boni et al., "A Broad Band Waveguide to Coaxial Transition for High Order Mode Damping in Particle Accelerator RF Cavities", Particle Accelerators, Vol. 45, 4 (1994), p. 195.

[5] G. Oxoby et al., "Bunch-by-Bunch Longitudinal Feedback System for PEP2", in Proceedings of the 4th EPAC, London, 27 June - 1 July, 1994, pp. 1616 - 1618.

[6] R. Boni et al., "A waveguide overloaded cavity as longitudinal kicker for the DAΦNE bunch by bunch feedback system", to be published in Particle Accelerators.

[7] Gallo et al., "Simulations of the Bunch-by-Bunch Feedback Operation with a Broadband RF Cavity as Longitudinal Kicker", DAΦNE Technical note G-31, Frascati, April 29, 1995.

[8] Corlett J. N. et al., "Longitudinal and Transverse Feedback Kickers for the ALS", in Proceedings of the 4th EPAC, London, 27 June - 1 July, 1994, p.1625.

[9] R. Boni et al., "Update of the Broadband to 50 Ω Coaxial Transition for Parasitic Mode Damping in the DAΦNE RF Cavities", in Proceedings of the 4th EPAC, London, 27 June - 1 July, 1994, p. 2004.

[10] Hewlett&Packard Co, "HFSS, the High Frequency Structure Simulator HP85180A^{TM}".

[11] Hahn H. and Pedersen F., "On Coaxial Wire Measurements of the Longitudinal Coupling Impedance", BNL-50870, UC-28, April 1978.

[12] M. Serio,"Feedback Status", 4th DAΦNE Machine Review, Frascati, January 19-20,1993.

[13] Goldberg-Lambertson, "Dynamic Devices: A Primer on Pickups and Kickers", LBL-31664, ESG-160.

[14] K.-Y. Ng, "Impedance of Stripline Beam Position Monitors", Particle Accelerators, Vol. 23, (1988), p. 93.

[15] R. Klatt et al., "MAFIA - A Three-Dimensional Electromagnetic CAD System for Magnets, RF Structures, and Transient Wake Field Calculations", SLAC report 303, 1986.

[16] F. Marcellini, M. Serio and M. Zobov, "DAΦNE Broad-band Button Electrodes", DAΦNE Technical note CD-6, Frascati, January 16, 1996.

[17] R. E. Shafer, "Characteristic of Directional Coupler Beam Position Monitors", IEEE Trans. on Nucl. Science, Vol. NS-32, No. 5, pp. 1933-1937.

[18] S. S. Kurennoy, "Polarizabilities of an Annular Cut and Coupling Impedances of Button-Type Beam Position Monitors", presented at the 16th IEEE PAC95 and ICHEA, Dallas, Texas, May 1-5, 1995; e - Print Archive: acc - phys/9504003.

[19] A. Gallo et al., "Impedance of DAΦNE Shielded Bellows", DAΦNE Technical note G-39, Frascati, March 29, 1996.

[20] M. Zobov et al., "Collective Effects and Impedance Study for the DAΦNE Φ-Factory", LNF-95/041 (P), 31 Luglio 1995.